CYCLIC FLEXURE TESTS OF MASONRY WALLS REINFORCED WITH GFRP SHEETS

Marc D. Kuzik[1], Alaa E. Elwi[2] , J.J. Roger Cheng[2]

ABSTRACT

The research work reported here investigates the out-of-plane flexural behavior of masonry walls reinforced externally with Glass Fiber Reinforced Polymer (GFRP) sheets and subjected to cyclic loading. Nine full-scale tests were performed in which three parameters were studied. These included the level of compressive axial load, amount of internal steel reinforcement, and amount of externally bonded GFRP sheet reinforcement. Of the three parameters studied, varying the amount of GFRP sheets was the only parameter that significantly affected the behavior of the walls. The GFRP sheet reinforcement governed the linear response of the bending moment versus centerline deflection hysteretic response. Increasing or decreasing the amount of GFRP sheet reinforcement either increased or decreased both the wall stiffness and ultimate strength respectively. Except for visible cracks, the walls maintained their structural integrity throughout the out-of-plane cyclic loading. The unloading/reloading paths for successive loading cycles were similar indicating little degradation. Thus, the general behavior of the walls was very predictable. The system, therefore, could be used to advantageously rehabilitate older masonry structures that are inadequately reinforced to withstand seismic events.

[1]Ph.D. Student

[2]Professor
University of Alberta
Edmonton, Alberta
Canada

INTRODUCTION

The use of FRP as external reinforcement for masonry walls was studied at various levels over the past few years. Ehsani *et al*. (1993) tested six masonry beams constructed from burned clay bricks in stack bond. FRP was bonded to the tension face of the beams and the load was applied at two points to create a region of zero shear. Triantafillou (1998) tested six clay brick masonry walls externally reinforced with unidirectional CFRP laminates in the out-of-plane direction. The walls had a cross section of 400 mm wide by 120 mm thick and a clear span of 780 mm. The CFRP was bonded on one side only and the loading was monotonic. The deflection response obtained was linear almost to the point of failure. Kolsch (1998) tested an external reinforcing system for masonry walls incorporating carbon fibre. The load was cycled monotonically using an air bag on one side of the wall. The load versus mid-height deflection showed a tri-linear behavior with little stiffness degradation in successive loading cycles. The specimens were typically able to withstand lateral loads equivalent to the inertial forces generated from 3g (gravity) acceleration.

In 1997, a research program at the University of Alberta (Albert et al. 1997) started to investigate the performance of masonry walls strengthened with Fibre Reinforced Polymers (FRP). Albert et al. (1998) reported a series of thirteen full-scale wall specimens reinforced with carbon fibre straps, carbon fibre sheets, and glass fibre sheets. These walls were loaded under monotonic, out-of-plane flexure. This series was ungrouted and no reinforcement other than the FRP was incorporated. The results successfully showed that externally applied FRP substantially increased the out-of-plane load resistance of unreinforced masonry walls under monotonic loading. The Albert et al. series showed a variety of failure modes including: fibre debonding, rupture of the sheets, and flexure-shear. The latter was characterized by diagonal cracks in the plane of the face shell adjacent to the FRP strips.

The research reported here extends the work of Albert et al. to include the behavior of lightly reinforced masonry walls built with hollow concrete blocks and fitted with GFRP sheets under fully reversed out-of-plane cyclic loading. At the time the Albert et al. tests were carried out, cost considerations showed a substantial advantage for the GFRP sheets as opposed to the carbon fiber based products. Ease of handling and shelf life considerations also seemed to favor GFRP sheets; hence the choice of sheets over straps and GFRP sheets over CFRP. This paper reports a phase of the research program in which a series of eight, full-scale masonry walls reinforced externally with GFRP sheet strips on both face shells was conducted. Each wall was 4 m tall and 1.2 m wide. The walls were tested in a vertical position under constant compressive axial load and increasing fully reversed cyclic out-of-plane lateral load. The lateral load was applied at two lines: 1200 mm from the top support and 1200 mm from the bottom support. The parameters investigated

included the amount of GFRP sheets, amount of steel reinforcement, level of axial load, and the behavior of bonded GFRP sheets under cyclic loading.

MATERIAL PROPERTIES

Five grouted and five ungrouted prisms were built during the construction of the wall specimens using 200 mm concrete masonry units and type S mortar to determine f'_m, the standard prism compressive strength of hollow concrete block masonry assemblies. Each prism was five courses high and one standard block wide. The compressive strength for ungrouted and fully grouted prisms was 10.33 MPa and 9.32 MPa respectively.

Tension tests were performed on both the 10M and 15M reinforcing steel bars. The yield strength for the 10M was 434 MPa with a modulus of elasticity of 200 GPa and the 15M had yield strength of 441 MPa with a modulus of 201 GPa.

The GFRP sheets used were SEH-51 with Tyfo® S epoxy. This material was supplied in a 1200 mm wide roll where the individual fibres were oriented uniaxially in the longitudinal direction with perpendicular cross weaves used to hold the longitudinal fibres in place. The SEH-51 was not pre-impregnated and was thus very flexible at the time of application. The material properties were determined from two GFRP sheet tension coupons made in accordance with ASTM D 3039-95a (1995). The cross sectional area of the tension coupons was calculated using the width and the thickness reported by the manufacturer for the pregnated sheets. Both tension coupon specimens successfully failed within the gauge length. Foil strain gauges were bonded to the coupons to provide strain readings and the load was measured through the MTS testing machine load cell. The tests showed an ultimate strain of 0.022 and a modulus of elasticity of 27,521 MPa.

TEST SPECIMENS

Eight masonry wall specimens were constructed by professional masons using 15 MPa, 200 mm standard concrete block and type S mortar. Each wall was 4.0 m (20 courses) tall and 1.2 m (two full blocks and one half block) wide. Horizontal joint reinforcement consisted of #9 gauge ladder type located at every third course. All specimens were built on 1200 mm x 200 mm x 51 mm steel plates for two purposes: to ensure an even load distribution at the bottom support, and to facilitate the attachment of a lifting device.

The primary variables of interest, listed in Table 1, were level of axial load, amount of steel reinforcement, and amount of GFRP sheets. After the walls were constructed, seven walls were each fitted with either two 10M or two 15M vertical reinforcing steel bars. One bar was placed in the second core from each side of the wall yielding a spacing of 600 mm on-center. The cores containing the vertical steel were then filled with grout. One wall specimen did not contain reinforcing steel and was not grouted.

EXTERNAL GFRP SHEET REINFORCEMENT

The reinforcement strategy was to apply GFRP sheets having equal cross-sectional area to both faces of a wall using the two-part high-strength high-modulus epoxy supplied with the GFRP sheets. All the GFRP sheets were oriented in the same

direction with the fibres spanning vertically. All sheets were applied to completely unloaded walls in a vertical position, so that there is no prestressing effects in sheets where axial loads present apriori, except for the own weight. Figure 1 shows the GFRP sheet layout schemes. The third column of Table 1 refers to the GFRP sheet arrangement. For example, Wall 1 is reinforced with two GFRP sheets on each face; each sheet is 250 mm wide. The primary scheme is that of Wall 1. In Walls 3 and 4 the sheet widths were varied. In specimens 5, 6 and 7, the axial force was varied. In Wall 8 the steel reinforcement was varied, and in Wall 2 no GFRP sheets at all were used. That last specimen was used for comparison purposes. Wall 5b was tested to cracking, with no FRP sheets, then unloaded, fitted with GFRP sheets and then tested again to failure.

TESTING PROCEDURE

The details of test frame were published earlier (Kuzik et al. 1999). Figure 2 shows the loading frame used for all the tests which provided a pin-pin type boundary condition. The instrumentation was designed to measure the deflected wall profile as well as the GFRP longitudinal strains.

The axial load was based on design dead and live loads from a one-storey warehouse type building in Vancouver, British Columbia, Canada. Rain and snow loads were chosen from this city since it is located in a zone of potentially high seismic activity along the west coast of North America.

The loading program for each specimen was divided into two phases. The first three groups of cycles were conducted under load control mode. The term “group” refers to a family of fully reversed complete cycles. Within each group, the walls were loaded to a predefined load level for three consecutive cycles. The load level for each group was calculated as a percentage of the predicted ultimate load obtained from a simple strain compatibility analysis. These levels in successive cycles were stepped up in increments of 25% of the predicted ultimate lateral load using the Albert et al. (1998) model.

The second stage of the lateral loading program for the walls was based on a centerline displacement criterion. A reference displacement was taken as the largest displacement experienced during the final group of load control cycles: group three. This reference displacement was divided by three and typically rounded up or down to the nearest multiple of 5 mm to obtain the incremental displacement required for subsequent loading cycles. Each group of displacement controlled cycles included one or two complete loading cycles to the specified displacement. This was continued until the ultimate capacity of the wall was obtained. Details of the load levels and the displacement control scheme have been published by Kuzik et al. (1999)

TEST OBSERVATIONS

All specimens tested showed consistent behaviour with clear trends. All specimens also failed by flexure shear failure above and below the load lines. In the following, a detailed description of the tests of specimens 5 and 1is provided. Other specimens are described in detail by Kuzik et al. (2000).

Wall 5a, 5b (Tests 1 & 2)

Two tests were performed on Wall 5. Specimen 5a was a control specimen and had no externally applied GFRP sheets but contained two 10M reinforcing bars. The lateral load consisted of thirteen cycles of which the first nine cycles were controlled by the level of lateral load and the remaining five cycles were controlled by level of centerline deflection. To obtain reasonable loading rates throughout the test, values of 1, 2, 4, and 10 mm/min of jack stroke were programmed into the signal generator. Load reversals were manually performed when either the desired level of load or centerline deflection was reached.

At this point, cracking occurred at the joint locations in the zero shear span (the test span). These cracks grew progressively larger as the level of lateral load was increased. On the thirteenth cycle, no increase in lateral load resistance was observed and the testing was stopped. This wall could have tolerated further deformations but it was desired to retrofit a partially damaged wall with externally applied GFRP sheets.

Wall 5a was then fitted with two 250 mm wide GFRP sheets on each side of the wall and retested as Wall5b. During the first loading cycle at 5.2 kN, the GFRP sheets spanning a bed joint on the compression side in the zero shear region began to buckle outwards. As the test progressed, local buckling of the GFRP sheets occurred at most bed joints in the zero shear span. When the lateral load on the wall was reversed, the buckles in the GFRP sheets gradually disappeared as the GFRP sheets began to stretch in tension. Cracking at the joints on the tension face was evident from the first cycle due largely to the fact that the wall was previously cracked. During the eleventh loading cycle, the jack stroke for both jacks exceeded the calibrated range. This resulted in both jacks continuing to travel to the fully extended position, which caused an unexpected catastrophic failure.

Wall 1 (Test 3)

Wall 1 was considered to be the standard wall from which all the testing parameters were varied. During the first group of loading cycles, hairline cracks developed at the mortar joints between the two vertical strips of GFRP sheet. By the third group of loading cycles, the mortar joints were fully cracked and there was no debonding or localized buckling of the GFRP sheets while under compression. Figure 3 shows some typical diagonal cracks forming in the masonry along each strip of GFRP sheet. These cracks started at the edge of the GFRP sheets about 50 mm from each bed joint and digressed at 45 degree angles to the bed joints. During the twelfth cycle, a vertical crack opened on the side of the block in the sixth course from the bottom, which induced the failure mode of flexure-shear. The testing was stopped at this point and the wall was returned to the zero position.

FLEXURE-SHEAR FAILURE MODE

As mentioned above, the only observed mode of failure was that of flexure-shear. This failure mode typically occurred simultaneously in the courses directly below the lower load line and directly above the upper load line. At these locations, the combination of shear force and curvature is at a maximum. The progression of this failure type is shown in Fig. 4. These cracks typically start at the bed joint to block interface at a depth equivalent to either half the wall width or the thickness of the face shell. Both of these locations can be viewed as regions of high stress concentration as there are radical changes within the cross-sectional geometry of the

masonry units. The cracks eventually cause the blocks to split and two pieces translate laterally away from one another. This translation, if large enough, begins to debond the GFRP sheets on the tension face within the shear span inducing a peel-off effect. In some specimens failure originated on the push side, in others on the pull side. Thus, the test set up was not a factor in the failure direction. The failure side was governed by which direction was incremented up first.

LOADING ENVELOPE RESPONSE

As an example, the total lateral load versus centerline deflection hysteresis for Wall 1 is shown in Fig. 5. The "pinched" response from these cyclically loaded specimens is relatively indistinguishable from that of a virgin specimen loaded monotonically (Albert *et al*. 1998). Assuming the response starts at the origin, it proceeds through a series of regions up to the point of failure. Qualitatively, the observed behaviour is slightly different form that obtained by Hamid *et al*. (1990) from fully reversed cyclic testing on six, masonry block walls. The wall tests reported in the current work showed little evidence of the flattening out of the unloading branch at low loads reported by Hamid. Rather an almost secant unloading path was observed. This suggests dominance of the FRP sheets behaviour over that of the reinforcing bars.

To understand the mechanisms affecting the shape of the loading envelopes, both the GFRP sheet strains and the steel reinforcement strains are analyzed. Figure 6(a), shows one-half of the bending moment versus deflection hysteresis from Wall 1, while Fig. 6(b) shows the corresponding GFRP sheet and steel reinforcement strains versus bending moment.

Figure 7 illustrates the points stated in the following discussion. Upon initial loading, the slope from the origin to the cracking moment, point *B*, is determined by the gross moment of inertia since the section is largely uncracked. The wall then cracks and the stiffness is slightly reduced. Up to point C there is no significant difference between the strain in the block or the joint.

A transition zone follows between C and *D*, in which a large discrepancy in strain between the face shell of the masonry immediately bonded to the GFRP sheets and the rest of the face shell, induces a shear strain field in the face shell evidenced by diagonal cracks in the face shell. The diagonal cracks are followed by horizontal cracks across the face shell itself. This phenomenon was reported by Albert *et al*. (1998).

The successive appearance of the shear lag cracks allows more of the GFRP sheet to directly experience strains that are larger than those normally tolerated by the blocks behind and adjacent to the GFRP sheet. Thus, as more of the GFRP sheet is gradually “mobilized” due to progressive shear lag cracking, the slope in region *C* to *D* decreases. This increase in GFRP sheet mobilization is analogous to a *system of rigid bodies connected by linear springs*. Figure 8 illustrates this analogy. It must be emphasized that the GFRP sheets stiffness does not change. Rather, more of the GFRP sheet is mobilized and thus the stiffness of the masonry/GFRP sheet reinforcement system decreases. In terms of the analogy above, longer and longer springs with the same spring constant are continuously substituted into the system.

At point *D*, the rate of increase in the GFRP sheet strain at the center-of-block location is approximately equal to the rate of increase in the GFRP sheet strain at the bed joint location. This is clearly shown in Fig. 7(b). At this point, a sufficient level

of cracking has occurred to stabilize the interaction between the GFRP sheets and the masonry on the tension face. Hence, the rest of the behavior up to failure is dominated by the GFRP sheet reinforcement on the tension face, which behaves linearly elastic to rupture, and by plastic strains within the bed joint on the compression face.

Up to point *E*, the tensile component of the internal moment resisting mechanism consists of both the GFRP sheets and the steel reinforcement. Once the steel yields, the tensile force in the steel remains constant, determined by the yield stress, while the tensile force in the GFRP sheet continues to increase; hence the slight decrease in slope at point *E*. Beyond point *E* to failure at point *F*, the envelope remains linear as the GFRP sheets on the tension side and the face shell on the compression side dominate the behavior.

The remaining region of the bending moment versus deflection envelope is the unloading/reloading from/to point *F* to *G*. The linear behavior of this region is totally controlled by the GFRP sheet reinforcement, which results in a very predictable and well-defined pattern. Because the GFRP sheet behaviour remains linear elastic until rupture, the material always unloads back to zero strain with no permanent deformation. Thus, upon unloading, the GFRP sheets fully closes all the cracks formed when the adjacent masonry face shell is in tension. Since the GFRP sheets are always bonded to the extreme tension face, the neutral axis remains closer to the geometric centroid throughout the cyclic loading history resulting in lower strains in the steel reinforcement. The benefit of both tensile resisting mechanisms remaining elastic during cyclic loading is very little loss of system integrity.

If the system integrity is maintained, then after unloading, the following reloading cycle occurs, more or less, along the previous unloading path. This behavior is well defined and thus, it can be easily and accurately predicted. As seen for a typical wall in Fig. 5, some damage does occur to the wall throughout the loading history as the unloading branches do not pass through the origin. This slight progressive lateral shift of the unloading branch indicates that some minor plastic behavior is occurring.

EFFECT OF WALL PARAMETERS

The parameters investigated in this program were the amount of steel reinforcement, amount of GFRP sheets, and level of axial load. Figure 8 shows a comparison of the bending moment versus centerline deflection envelopes for each of the parameter groups. The only parameter that significantly altered the behavior was the amount of GFRP sheet reinforcement as shown in Fig. 8(b). Three noticeable effects occurred as the amount of GFRP sheet was reduced while both the amount of steel reinforcement and level of axial load remained constant.

Both the transition moment and the ultimate moment were progressively reduced as the amount of GFRP sheet was reduced. As the area of the GFRP sheet is reduced, so is the internal tensile force provided by the GFRP sheet to balance the forces within the cross-section during flexural loading. Since the internal moment arm of the GFRP sheet is more than double the internal moment arm of the steel reinforcement, the resisting moment of the section is more sensitive to the force component provided by the GFRP sheet. When initial cracking occurs, strains are mobilized only in a highly localized region of the GFRP sheet directly adjacent to the crack. As the amount of GFRP sheet is reduced, the average strain increases for a given moment, thus requiring the crack width to become larger. Hence, the transition moment reduces as a result of the decreasing ability of the GFRP sheet to

prevent crack propagation. At the ultimate moment condition, the reinforcing steel has yielded and thus its contribution towards equilibrium of the internal forces is constant. Since the GFRP sheets remains linearly elastic until it ruptures, the internal force contribution from the GFRP sheet is directly proportional to its area. The ultimate moment is, thus, controlled by the maximum force mobilized in the GFRP sheet, which decreases as the area decreases.

The third behavioral difference is the stiffness after the transition moment. This is a direct effect of the cross-sectional properties, namely the cracked moment of inertia. In calculating the cracked moment of inertia about the geometric centroid of the cross-section, only the GFRP sheet in tension and the masonry above the neutral axis contribute significantly. As the crack depth increases, the contribution of the masonry towards the moment of inertia reduces, whereas the contribution from the GFRP sheet remains constant. Thus, the effective cracked stiffness of the cross-section depends heavily on the amount of bonded GFRP sheet.

For the wall specimens fitted with either 130 mm wide or 250 mm wide GFRP sheets, some localized buckling of the GFRP sheets occurred at the bed joint locations. However, buckling of the 65 mm wide GFRP sheets occurred over the center of the masonry blocks, not over the bed joints. As discussed previously, the progressive cracking of the masonry is a result of the internal force interaction between the GFRP sheets and the masonry. The critical link between the GFRP sheet and the masonry is the bond provided by the epoxy. For wider GFRP sheets, the shear stress developed between the GFRP sheets and the masonry does not exceed the epoxy bond stress. Rather, the masonry tensile strength is first exceeded resulting in the masonry cracking before debonding of the GFRP sheets occurs. Conversely, for the narrow GFRP sheets, an insufficient bond width/area is provided to transfer the tensile forces from the GFRP sheet to the masonry at the center-of-block location.

CONCLUSIONS

The overall flexural performance of the masonry walls reinforced externally with GFRP sheets was excellent. Except for visible cracks, the walls maintained their structural integrity throughout the out-of-plane cyclic loading. Quantitatively, the integrity of the GFRP sheets/masonry wall system is maintained as shown through the load versus deflection hysteretic responses. The unloading/reloading paths for successive loading cycles were similar indicating little degradation. In addition, all the unloading paths pass near the origin resulting in a pinching effect that again indicates little degradation of the wall system. Thus, the general behavior of the walls was very predictable. The system, therefore, could be used to advantageously rehabilitate older masonry structures that are inadequately reinforced to withstand seismic events.

An envelope with three distinct regions provides a boundary for the bending moment versus centerline deflection response. The first region had a linear slope that ends at the cracking moment. This is followed by a transition zone through which progressive debonding of the sheets at the joints is observed. Following that a stable zone is reached during which progressive debonding through the blocks is observed. The third region bounds the unloading response, which again followed a secant linear path in which the slope is governed by the progressive damage described above.

Of the three parameters studied, varying the amount of GFRP sheet was the only parameter that significantly affected the behavior of the walls. The GFRP sheet reinforcement governed the linear response of the bending moment versus centerline deflection hysteresis. Increasing or decreasing the amount of bonded GFRP sheet reinforcement either increased or decreased both the wall stiffness and ultimate strength respectively.

ACKNOWLEDGEMENTS

This work was conducted in the course of research leading to a Master of Science degree for the first author. The research was funded in part by the Canadian Masonry Research Institute (CMRI), the Network of Centre of Excellence on Intelligent Sensing For Innovative Structures (ISIS), and the Natural Sciences and Engineering Research Council of Canada (NSERC).

REFERENCES

Albert, M.L., Cheng, J.J.R., and Elwi, A.E. (1998). Rehabilitation of Unreinforced Masonry Walls with Externally Applied Fiber Reinforced Polymers, Struct. Eng. Rep. No. 226, University of Alberta, Edmonton, T6G 2G7.

Ehsani, M.R., Saadatmanesh, H., Abdelghany, I.H., and Elkafrawy, W. (1993). "Flexural Behavior of Masonry Walls Strengthened with Composite Fabrics," ACI Int. Symp. on FRP Reinforcement for Concrete Structures, Vancouver, Canada, ACI SP-138, pp. 497-507.

Hamid, A.A., Abboud, B.E., Farah, M., and Harris, H.G. (1989). "Flexural Behavior of Vertically Spanned Reinforced Concrete Block Masonry Walls," Proc. of the 5th Canadian Masonry Symp., June 5-7, University of British Columbia, Vancouver, Vol. 1, pp. 209-218.

Hamid, A.A., Hatem, M.K., Harris, H.G., and Abboud, B.E. (1990). "Hysteretic Response and Ductility of Reinforced Concrete Masonry Walls under Out-of-Plane Loading," Proceedings of the Fifth North American Masonry Conference, University of Illinois at Urbana-Champaign, Vol. I, pp. 397-405.

Kolsch, H. (1998). "Carbon Fiber Cement Matrix (CFCM) Overlay System for Masonry Strengthening," Journal of Composites for Construction, ASCE, 2(2), pp. 105-109.

Kuzik, M.D., Elwi, A.E., and Cheng, J.J.R. (1999). Out-of-Plane Cyclic Behavior of Masonry Walls Reinforced Externally with GFRP, Structural Engineering Report No. 228, University of Alberta, Edmonton, T6G 2G7.

Neale, K.W. (1999). "FRPs for Structural Rehabilitation: A survey of Recent Progress," Progress in Structural Engineering and Materials, *in press*.

Triantafillou, T.C. (1998). "Strengthening of Masonry Structures Using Epoxy-Bonded FRP Laminates," J. of Composites for Construction, ASCE, 2(2), pp. 96-104.

Table 1. Test Specimen Parameters and Results

	Steel Rfmt.	GFRP width/side (mm)	Axial Load (kN)	Number of Full Cycles	Ultimate Load (kN)	Ultimate Deflection (mm)	Failure Mode
Wall 1	2-10M	(2 x 250)	28.61	12.5	57.1	98.9	Flexure-shear
Wall 2	none	(2 x 250)	31.75	15.5	38.1	82.3	Flexure-shear
Wall 3	2-10M	(2 x 125)	30.13	13.5	39.0	122.2	Flexure-shear
Wall 4	2-10M	(2 x 65)	30.16	13.5	28.4	137.0	Serviceability
Wall 5a	2-10M	none	32.07	15	15.2	58.9	Flexure-shear
Wall 5b	2-10M	(2 x 250)	30.81	10.5	53.2	88.6	Flexure-shear
Wall 6	2-10M	(2 x 250)	15.45	12.5	65.3	113.5	Flexure-shear
Wall 7	2-10M	(2 x 250)	46.54	13.5	69.1	118.0	Flexure-shear
Wall 8	2-15M	(2 x 250)	29.36	13.5	84.1	132.0	Flexure-shear

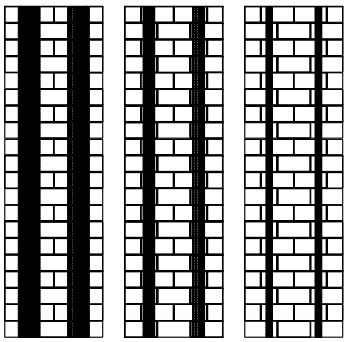

Figure 1. GFRP Sheet Arrangement

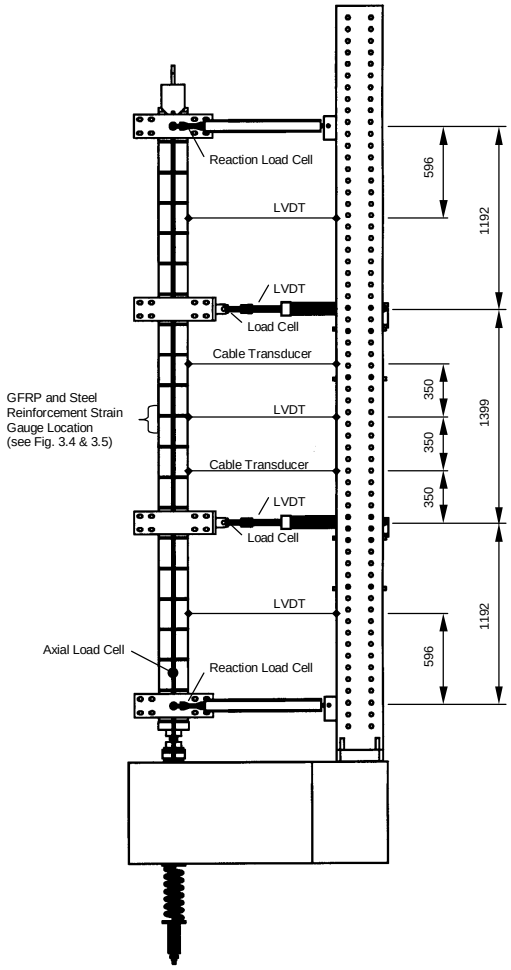

Figure 2. Test Setup

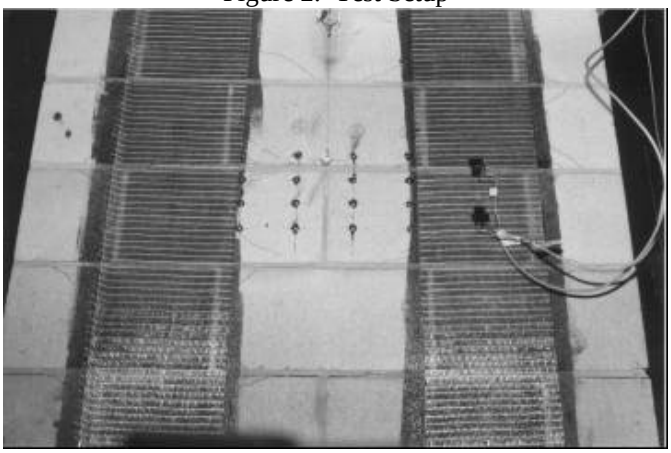

Figure 3. Diagonal Shear Lag Cracks Adjacent to GFRP Strips

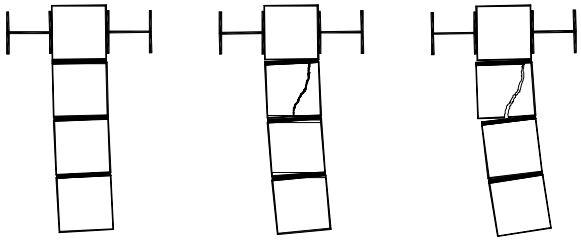

Figure 4. Progression of Flexure Shear Failure

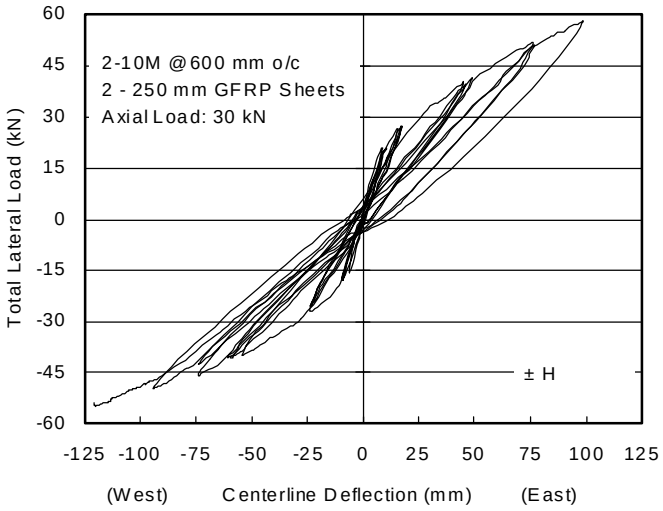

Figure 5. Load Deflection Response of Wall 1

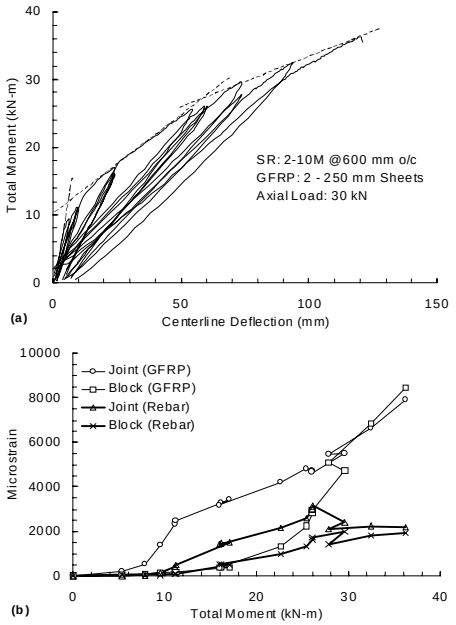

Figure 6. (a) Moment and (b) Strain Responses of Wall 1

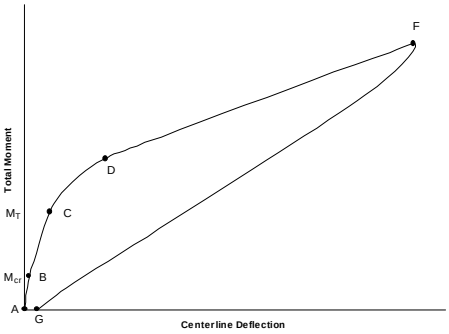

Figure 7. Defined Points on the Response

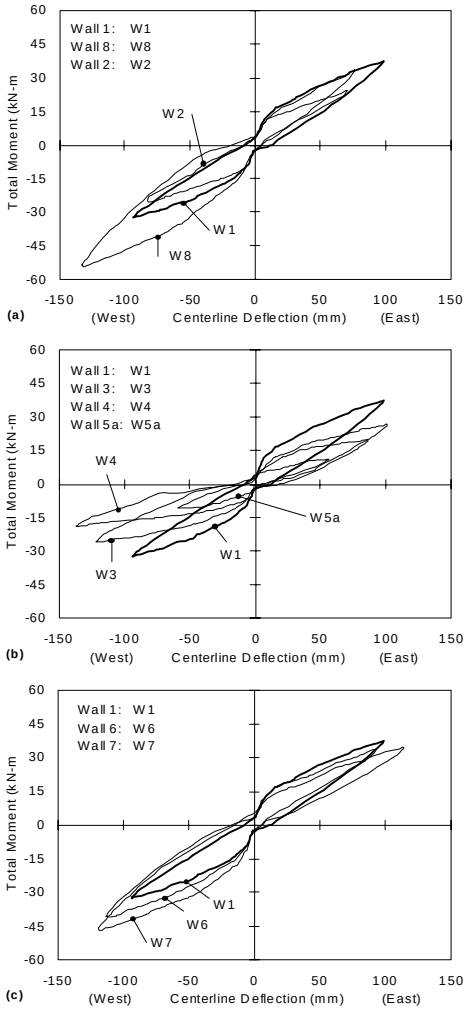

Figure 8. All Envelopes
(a) Walls 1, 2, 8
(b) Walls 1, 3, 4, 5a
(c) Walls 1, 6, 7